ARTICLE

doi:10.1016/S1525-0016(03)00037-6

Targeted Delivery of DNA to the Mitochondrial Compartment via Import Sequence-Conjugated Peptide Nucleic Acid

A. Flierl,[1,*] C. Jackson,[2] B. Cottrell,[1,*] D. Murdock,[1,†] P. Seibel,[3] and D.C. Wallace[1,‡]

[1]*Center for Molecular and Mitochondrial Medicine and Genetics (MAMMAG), University of California, Irvine, 2122 Natural Sciences I, Irvine, California 92697-3940, USA (formerly Center for Mitochondrial Medicine, Emory University)*
[2]*Research Genetics, 2130 Memorial Parkway SW, Huntsville, Alabama 35801, USA*
[3]*Biozentrum der Universitaet Wuerzburg, Lehrstuhl fuer Zell- und Entwicklungsbiologie (Zoologie I), Am Hubland, 97074 Wuerzburg, Germany*

**Current address: Buck Institute, 8001 Redwood Blvd., Novato, California 94945, USA.*

†Current address: Division of Medical Genetics, DD-2205 Medical Center North, VUMC, Nashville, Tennessee 37232, USA.

‡To whom correspondence should be addressed. E-mail: dwallace@uci.edu.

We report that oligonucleotides can be introduced into the mitochondria of living mammalian cells by annealing them to peptide nucleic acids coupled to mitochondrial targeting peptides. These complexes are imported into the mitochondrial matrix through the outer and inner membrane import channels of isolated mitochondria. They are also imported into the mitochondria of cultured cells, provided that the cytosolic uptake of the complexes is facilitated by using synthetic polycations or membrane permeabilizing toxins. Our method now promises to provide a viable strategy for the genetic modification of the mitochondria in cultured cells, animals and patients.

Key Words: mitochondria, transformation, import, targeting peptide, peptide nucleic acid, drug delivery, oligonucleotide, gene therapy

INTRODUCTION

No routinely successful method has been developed for introducing exogenous DNA into the mitochondria of living mammalian cells. To reach the mitochondrial matrix where the mitochondrial DNA (mtDNA) resides, the exogenous DNA must traverse three membranes: the plasma membrane, the mitochondrial outer membrane and the mitochondrial inner membrane.

DNA has been introduced into the mitochondria of plant cells and yeast by biolistic transformation (1), though this procedure has not been productive for mammalian cells. DNA has been introduced into isolated mammalian mitochondria by electroporation (2), but there are no reports of repopulation of mammalian cells with electroporated mitochondria. Mitochondria isolated from somatic cells have been microinjected into cultured cells or oocytes (3), but this method uses naturally occurring mitochondrial genotypes and microinjection is impractical for the genetic manipulation of large numbers of cultured cells or for mitochondrial gene therapy in animal or human tissues.

DNA has also been introduced into isolated mitochondria by covalent-linkage of either oligonucleotides (4) or double stranded DNA (5) to N-terminal mitochondrial protein targeting peptides. Such conjugates are imported into the mitochondria via the "transport through the outer membrane" (TOM) and "transport through the inner membrane" (TIM) multi-protein import channel complexes (6). When fluorescently labeled short oligonucleotides, covalently linked to a mitochondrial targeting peptide, were introduced into cultured fibroblasts using liposomes, the fluorescence became associated with mitochondria-like structures. However, the matrix localization of the oligonucleotides was not established (7).

As an alternative to DNA, peptide nucleic acids (PNAs) (8) have been tried. PNAs use a peptide bond backbone instead of the sugar phosphate backbone of DNA or RNA

Abbreviations: DIG: Digoxigenin; FAM: Carboxy-fluorescein; mtDNA: mitochondrial DNA; nps: nucleotide pairs; PNA: Peptide Nucleic Acid; PPO: Peptide-PNA/oligonucleotide: SL-O: Streptolysin-O; TBE: Tris-Borate-EDTA; TG-SDS: Tris-Glycine-Sodiumdodecylsulfate.

1525-0016/03 $30.00

TABLE 1: Sequence and composition of conjugates and oligonucleotides

M conjugate	^{NH2}-MALLRGVFIVAAKRTPF-o-o-^{N}-GATTCTTCACCGT-^{C}
M oligonucleotide	$^{\#5'}$-*GGACT**ACGGTGAAGAATC-$^{3'}$
SCR conjugate	^{NH2}-HTSVVRNFWYGQPVQ-o-o-^{N}-GATTCTTCACCGT-^{C}
Y conjugate	^{NH2}-MLSLRQSIRFFKPAT-o-o-^{N}-TTCCTCGCTCACT-^{C}
Y oligonucleotide	$^{\#5'}$-*GAGTC**AGTGAGCGAGGAA-$^{3'}$

Sequence and composition of PNA–peptide conjugates and complementary oligonucleotides PNA–peptide/oligonucleotide complexes were formed by hybridization of PNA–peptide conjugates with their corresponding oligonucleotides. M conjugate, signal sequence of the mouse mitochondrial thiolase gene conjugated to a PNA complementary to mtDNA (*see Materials and methods*). SCR conjugate, scrambled peptide sequence conjugated to the same PNA sequence as the M conjugate. Y conjugate, signal sequence of yeast COX subunit IV conjugated to a PNA complementary to a commercial cloning vector. Superscript, orientation of peptides, oligonucleotides, and PNAs. -o-o-, linkers, connecting peptide and PNA moiety of the conjugate.

*Sequence in italics depicting 5′ overhang of oligonucleotides.

#Site of modification.

to connect nucleic acid bases. PNAs have been conjugated to N-terminal mitochondrial targeting peptides and these are imported into the mitochondria. However, PNAs cannot be incorporated into the mtDNA and could not be shown to affect gene expression in cells (9).

While apparently biologically inactive in themselves, PNAs have a very high affinity for base pairing with homologous oligonucleotides. This is because the peptide backbone eliminates the inter-strand repulsion that destabilizes double stranded nucleic acids (10). Moreover, PNAs are very stable in biological systems (11,12).

We now report combining these various strategies into a successful method for introducing oligonucleotides into the mitochondria of living cells. An N-terminal mitochondrial targeting peptide is covalently coupled to a PNA encoding a portion of the sequence to be introduced into the mitochondrion. This targeting peptide-PNA conjugate is then annealed to an oligonucleotide with the desired sequence and the complex transferred into the cytosol using either polycations or transient membrane channels. This procedure efficiently delivered labeled oligonucleotides into the mitochondrial matrix, both *in vitro* and *in vivo*.

RESULTS

Preparation of PNA-Peptide/Oligonucleotide (PPO)-Complexes

When PNA-peptide conjugates (Table 1) were annealed to a 100-fold molar excess of fluorescein (FAM), digoxigenin (DIG) or gold-labeled oligonucleotide (Table 1), more than 90% of PNA-Peptide conjugates were recovered as PNA-peptide/oligonucleotide (PPO) complexes (Fig. 1A). Formation of PPO-complexes could be confirmed by separation of reaction products in TBE-Urea or TG-SDS-polyacrylamide gel systems. However, due to the different physical and chemical properties of different labels on the oligonucleotides and the chimeric nature of PNA-peptides, no single gel system proved to be optimal for all of the chimeric constructs and complexes. Therefore, products were purified by HPLC (Fig. 1B and C) and recovered in HBS or PBS for application to mitochondria or cells.

Import of PPO-Complexes into Isolated Mitochondria

PPO-complexes bearing DIG-labeled oligonucleotides were selectively taken up by isolated mouse liver mitochondria, and detected using anti-DIG antibodies. For PPO-complexes encompassing a yeast COX IV pre-peptide conjugated to a PNA (Y-conjugate), labeled oligonucleotides were detected primarily in the inner membrane and in the matrix (Fig. 2) of mitochondria. Similar results were obtained for PPO-complexes using a mouse thiolase pre-peptide PNA-conjugate (M-conjugate).

The requirement for a normal N-terminal targeting peptide (Y- or M-conjugate) for import of the PPO-complexes through the TOM-TIM channels and into the matrix was confirmed by replacing the normal targeting peptide with a randomized (scrambled) amino acid sequence (SCR-conjugate). The SCR-conjugate/PPO-complex gave only a weak interaction with the outer mitochondria membrane and no oligonucleotides were detected in the inner membrane or matrix fractions (Fig. 2). Free oligonucleotides did not associate with the mitochondrial membranes at all.

The uptake of the PPO-complexes was about 50 fold higher with mitochondria energized by ATP then with ATP-depleted mitochondria (Fig. 2), and the uptake was five times more rapid for the Y-conjugate/PPO-complexes than for the M-conjugate/PPO-complexes, as quantified by direct comparison of in vitro import into the mitochondrial matrix. Thus, the PPO-complexes are taken up by the mitochondria via targeting sequence-specific active transport.

Uptake of Y-Conjugate/PPO-Complexes into Mouse Muscle Myoblast Cells

PPO-complexes were next used to treat cultured mouse C2C12 myoblasts. The mitochondrial uptake of the Y-

doi:10.1016/S1525-0016(03)00037-6

conjugate/PPO-complexes was compared with control SCR-conjugate/PPO-complexes.

To facilitate introduction of the PPO-complexes into the cell cytoplasm, four different protocols were tried: direct exposure, encapsulation in liposomes, aggregation with polycations, or diffusion through transient plasma membrane pores generated by Streptolysin-O (SL-O). To monitor the oligonucleotide fate, the 5′ ends were labeled with either fluorescein (FAM) or colloidal gold.

Passive Uptake of Mitochondrial-Targeted PPO-Complexes

Initially, 1 μM PPO-complexes containing 1 μM of FAM-labeled oligonucleotide (13) were apply directly to the myoblasts. At 30 min after exposure, myoblasts exposed to either PPO-complexes or free oligonucleotides showed intense, uniform, intracellular cytosolic fluorescence. By 1 hour after exposure the PPO-complex-associated oligonucleotide fluorescence was concentrated around the mitochondria with low cytoplasmic background (comparable to Fig. 3D), while free oligonucleotide fluorescence was faint and dispersed throughout the cytoplasm.

High magnification fluorescent microscopy (up to 1250x) did not reveal any indication for staining of organelles other than the mitochondria in the focal plane used, when comparing the fluorescence patterns generated by the PPO-complexes and Mitotracker®. Hence, cells are capable of taking up naked PPO-complexes and transporting them to the mitochondria.

To analyze the efficacy of introducing the PPO-complexes through the plasma membrane by liposomes, polycations, or SL-O pores; we reduced the PPO-complex concentration and thus the labeled oligonucleotide to 10 nM. This eliminated the background associated with the passive uptake of PPO-complexes observed at 1 μM.

Lipotransfection

Liposomes (14) proved unsuitable for introduction of the PPO-complexes into the myoblast cytoplasm. After liposome-facilitated transformation, the fluorescence of liposome-encapsulated PPO-complexes with targeting peptides, either Y-conjugate or SCR-conjugate, remained associated with the outside of the cell (Fig. 3C). This suggests that the hydrophobic targeting peptides became dissolved in the lipid bi-layer of the liposome and the plasma membrane rendering them inaccessible to the mitochondria. Indeed, cytosolic fluorescence was higher with liposome encapsulated oligonucleotides alone (Fig. 4A) or PPO-complexes lacking a targeting peptide (data not shown).

PEI-PPO-Complex Aggregate Transformation

The cytosolic delivery of PPO-complexes using branched chain polyethylenimine (PEI) was more successful. PEIs aggregate DNA, protecting it from endocytosis and endosomal degradation (15,16).

The optimal PEI molecular weight for PPO-complex delivery was 25 kDa and the optimal DNA to PEI ratio (N/P ratio) was 10/1. This created aggregates of 150–300 nm with the maximum DNA fluorescence.

Exposure of myoblasts to PEI-PPO-complex aggregates containing 10 nM of oligonucleotides resulted in the efficient uptake of PEI-PPO complex aggregates into the cytosol. Initially the PPO-complexes were distributed peri-nuclearly and co-localizing with the lysosome-specific dye Lysotracker™ (Fig. 3C). Subsequently, the oligonucleotide fluorescence became localized in bead-like structures of reduced size, creating a pattern in which some fluorescence remained co-localized with Lysotracker™, but most of the fluorescence co-localized with Mitotracker® (Fig. 3A) and similar to Fig. 3D. Thus, Y-conjugate/PPO-complexes were transferred from the lysosomal PEI-PPO-complex aggregates to the mitochondria.

The intensity of the mitochondrial oligonucleotide fluorescence was directly related to the proximity to the PEI-PPO-complex aggregates to the mitochondria. Mitochondria near the PEI-PPO-complex aggregates rapidly developed high-level fluorescence. The fluorescence then diffused along the mitochondria creating a fluorescent mitochondrial network, which was maintained for extended periods of time (Fig. 4B).

While mitochondrial uptake was intense with the Y-conjugate, it was absent with either the SCR-conjugate (Fig. 3A, SCR) or with PNAs lacking a targeting peptide (Fig. 3A {-pept} and Fig. 3B), indicating that the targeting peptide sequence was essential for mitochondrial uptake. Surprisingly, the SCR-conjugate/PPO-complex resulted in intense nuclear fluorescence (Fig. 3A, {SCR}).

It is unlikely that the Y-conjugate/PPO-complexes were simply stuck in the mitochondrial import channels, since the transfected cells did not show increased rates of cell death or in apoptotic changes in mitochondrial morphology such as fragmentation or “curling” of the mitochondrial network. Furthermore, the mitochondrial fluorescence diffused away from the PEI-PPO-complex aggregates along the mitochondrial network as if moving through an aqueous phase. Hence, it is most likely that the labeled oligonucleotides became localized in the mitochondrial matrix.

Streptolysin-O (SL-O) Permeabilization

PPO-complexes were also delivered to the cytosol using an optimized concentration of the bacterial toxin SL-O, which generates transient plasma membrane pores of up to 30 nm (17,18) (Fig.4a). Within 30 min after SL-O and Y-conjugate/PPO-complex treatment of the myoblasts, oligonucleotide fluorescence co-localized with Mitotracker® (Fig. 3D) and was uniformly distributed throughout the mitochondria. While the oligonucleotide fluorescence per mitochondrial unit was lower with SL-O than for mitochondrial adjacent to PEI aggregates, a much larger proportion of the mitochondrial network became

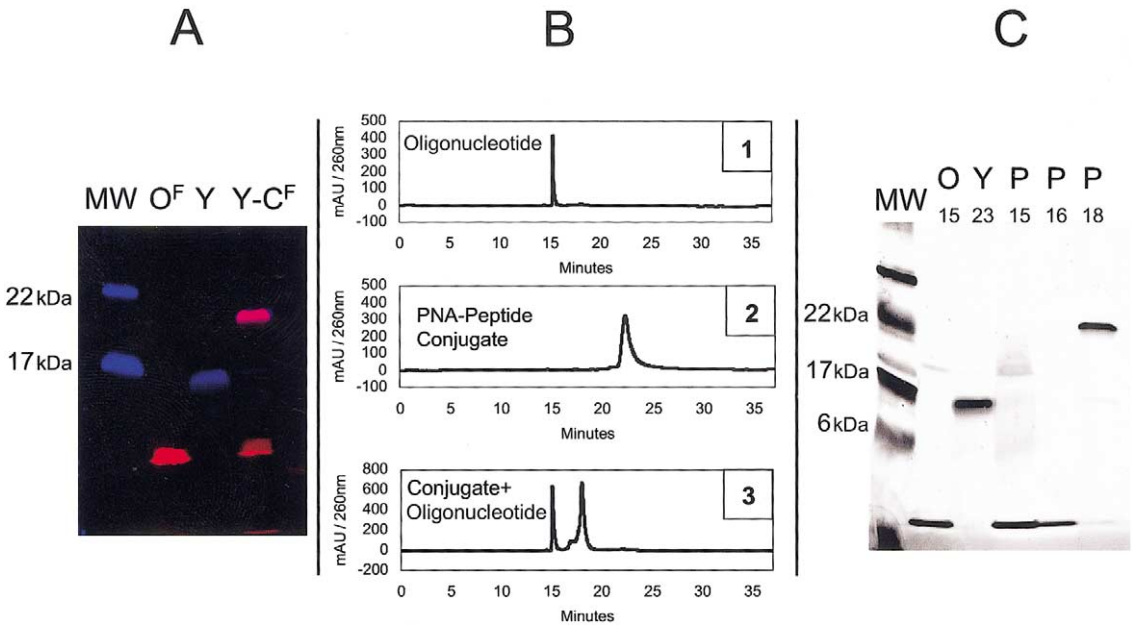

FIG. 1. Synthesis and purification of PNA-peptide conjugates and PPO-complexes. A, False color image of reaction products obtained by hybridization of the Y-conjugate containing a fluorescent-labeled PNA-peptide (Y) with FAM-labeled oligonucleotide (O^F) resulting in a fluorescent PPO-complex (Y-C^F) and separated by 15% TBE-Urea PAGE. MW: Molecular weight standard. B, HPLC profiles obtained from: 1. DIG-labeled oligonucleotide (O), 2. PNA-Y peptide conjugate (Y) and 3. the products of the completed hybridization reaction between PNA-peptide conjugate and labeled oligonucleotide (P). C, Peak fractions at indicated collection times (min) from B, separated as under A and detected by silver staining: lane 1 (O,15), 2 (Y,23) and 3–5 (P, 15; P,16; P,18). The intact PPO-complex is found in lane 5 (P,18).

fluorescent with SL-O. Therefore, the overall mitochondrial uptake of the Y-conjugate/PPO-complex per cell was higher using SL-O than PEI (Fig. 4B).

Following introduction by SL-O, the Y-conjugate/PPO-complexes gave intense mitochondrial fluorescence, while SCR-conjugate/PPO-complexes gave only nuclear fluorescence (similar to Fig. 3A). Following SL-O-stimulated Y-conjugate/PPO-complex exposure, the mitochondrial fluorescence slowly declined, suggesting that the labeled oligonucleotides in transformed mitochondria

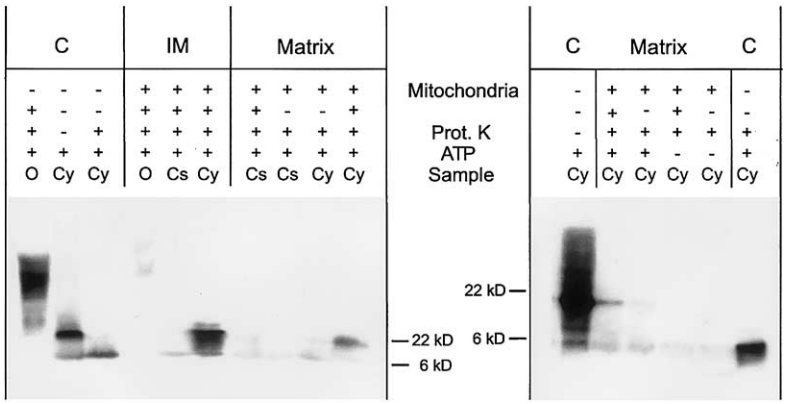

FIG. 2. Import of PPO-complexes into isolated mitochondria. DIG-labeled PPO-complexes in the post-mitochondrial supernatant (C), inner mitochondrial membrane fraction (IM), and mitochondrial matrix fraction (Matrix) were separated by 18% TG-SDS PAGE and detected by anti-DIG antibody after western transfer. Arrows indicate size of full length PPO-complex, which migrates at about 22 kDa. Complexes without signal peptide migrate at 6 kDa. The DIG-labeled oligonucleotide (O) migrates more slowly than oligonucleotides annealed to either the Y-conjugate/PNA or PNA alone; Cy: Y-conjugate hybridized to the labeled oligonucleotide (Y-conjugate/PPO-complex); Cs: SCR-conjugate hybridized to the DIG-labeled oligonucleotide (SCR-conjugate/PPO-complex). Reaction conditions: Mitochondria: (+ added/− not added); $\Delta\psi$: Mitochondrial membrane potential (+ intact/− dissipated by addition of proton ionophore FCCP); Prot. K: Proteinase K (+ added after import/− not added); ATP: (+ added/− not added).

doi:10.1016/S1525-0016(03)00037-6

were degraded by proteolytic or nucleolytic processes in the mitochondrial matrix (Fig. 4B). This contrasts to the stability of the PEI-PPO-complex aggregate mitochondrial fluorescence (Fig. 4B). Perhaps the stability of the mitochondrial fluorescence associated with the PEI-PPO-complex aggregates results from the continuous release of the Y-conjugate bound oligonucleotide into the cytosol, which replenishes the degraded mitochondrial oligonucleotides.

Electron Microscopy

The deposition of the oligonucleotides from the Y-conjugate/PPO-complexes into the mitochondrial matrix of the myoblasts was confirmed using Undecagold™-labeled oligonucleotides. At 30 minutes after exposure to PEI-PPO-complex aggregates, gold particles were observed by electron microscopy in cytoplasmic aggregates, presumably endolysosomes, as well as in association with the mitochondria (Fig. 5B). Within 4 hours of exposure, single Undecagold™ particles were observed in the mitochondrial matrix (Fig. 5A and C). Undecagold™-labeled oligonucleotides annealed to the SCR-conjugate or to PNAs without a targeting peptide were not detected either inside or near the mitochondria. While the efficiency of mitochondrial import of Undecagold™-labeled oligonucleotides is generally reduced (19), this result confirms that the Undecagold™-labeled oligonucleotides are transported into the mitochondrial matrix where they could then interact with the mtDNA.

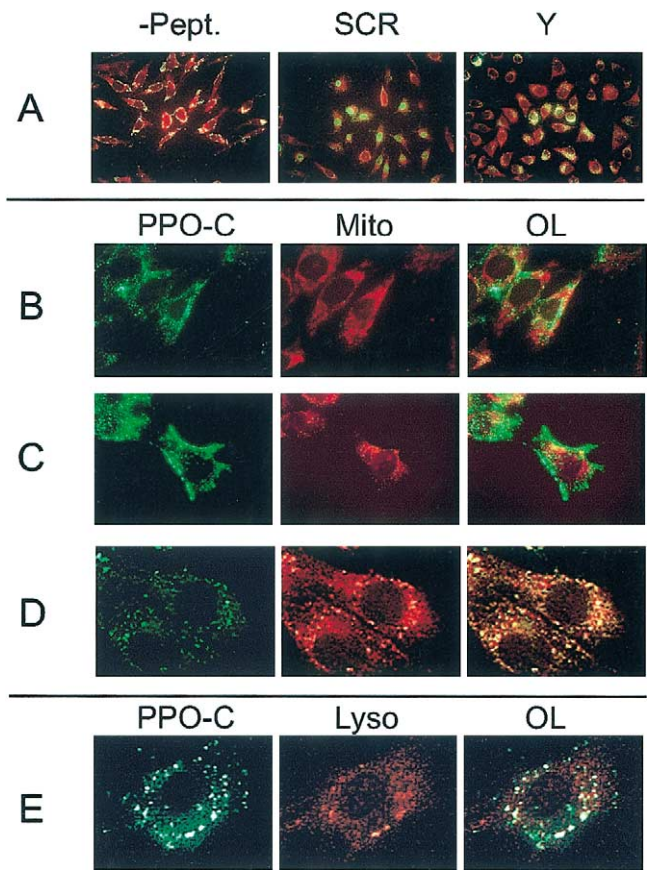

FIG. 3. Fluorescence microscopy of PPO-complexes in cultured myoblasts. *Panel A*: Cellular localization of the FAM-labeled oligonucleotide (green fluorescence) hybridized to PNAs conjugated to (from left to right) no peptide (-Pept.), SCR-conjugate (SCR), Y-conjugate (Y) and transformed by PEI. Mitochondria were counterstained with Mitotracker® (red fluorescence). Photomicrographs (240 ×) were taken 4 hrs after transformation. *Panels B–E:* Subcellular localization of FAM-labeled PPO-complexes in cultured cells. Labeling and detection of constructs and counterstaining of mitochondria was as in *Panel A,* unless stated otherwise. Depicted on each row are from left to right: FAM- fluorescence of PPO-complex (PPO-C), mitochondrial fluorescence by Mitotracker® (Mito), overlay of both channels (OL). *B:* Polyethylenimine (PEI) transformation using a PNA without signal peptide. *C:* Lipotransfection with the Y- conjugate/PPO-complex. *D:* Transformation with the Y-conjugate/PPO-complex by SL-O permeabilization. *Panel E:* Transformation of Y-conjugate/PPO-complex aggregated with PEI (PPO-C) and counterstained with Lysotracker™ (Lyso), staining the lysosomal compartment. OL: Overlay.

DISCUSSION

Many attempts have been made to develop a reliable method for delivering DNA to the mitochondrial matrix from outside a mammalian cell, but to no avail. Now, however, we report the successful import of labeled DNA oligonucleotides into the mitochondrial matrix using PNAs conjugated to mitochondrial targeting peptides as vehicles for the transport of annealed oligonucleotides through the TOM-TIM protein import apparatus.

Proof that we have succeeded in introducing native DNA oligonucleotides into the mitochondrial matrix of living cells comes from several interrelated observations. First, we showed that isolated mitochondria could take up Y-conjugate/PPO-complexes into the mitochondrial inner membrane and matrix. Second, we demonstrated that uptake of the PPO-complexes required energized mitochondria and a legitimate mitochondrial targeting peptide. Third, we showed that Y-conjugate/PPO-complexes within myoblasts were localized in structures that had the morphology of mitochondria and co-localized with Mitotracker®. Fourth, we demonstrated that Y-conjugate/PPO-complexes containing gold-labeled oligonucleotides were localized within the mitochondrial matrix as revealed by electron microscopy. Finally, we showed that the mitochondrial uptake within cells did not occur unless we used a functional mitochondrial targeting peptide.

Having developed an effective system for introducing oligonucleotides through the mitochondrial membranes and into the matrix, we increased the efficiency of mitochondrial transformation by using PEI aggregates or SL-O channels to enhance cellular uptake of the PPO-complexes. SL-O uptake gave the highest overall mitochondrial fluorescence, but then slowly faded. PEI aggregates gave intense regional mitochondrial fluorescence, and the

fluorescence was maintained longer. Hence, both methods may have merit in different contexts.

While considerable effort has been invested in optimizing our procedures, additional improvements may still be possible in the PPO-complex construction. Alternatives to the yeast COX IV mitochondrial targeting peptide may be more efficacious in mediating PNA/oligonucleotide uptake into the mitochondria (20) or may allow import of longer oligonucleotides. Modifications of the length and sequence of the PNA and the annealed oligonucleotide may enhance biological activity. The reason for the decline of the mitochondrial oligonucleotide fluorescence in the mitochondrial matrix needs to be determined and inhibited.

Still, having succeeded in introducing oligonucleotides into the mitochondria, we can now attempt to genetically modify the mtDNA. For example, an oligonucleotide could be introduced into the mitochondrial matrix that contains the base change in the 16S rRNA gene conferring resistance to the mitoribosome inhibitor chloramphenicol (CAP) (21). If this oligonucleotide can act as a primer for mtDNA synthesis, it could generate a mtDNA harboring the CAP resistant mtDNA mutation.

Thus, our approach now has the potential of introducing a wide variety of mtDNA mutations into mammalian cell and animal tissue mtDNAs. This should permit generation of specific models for mtDNA disease, and raises the possibility of correcting pathogenic mtDNA mutations in cells or animals (22).

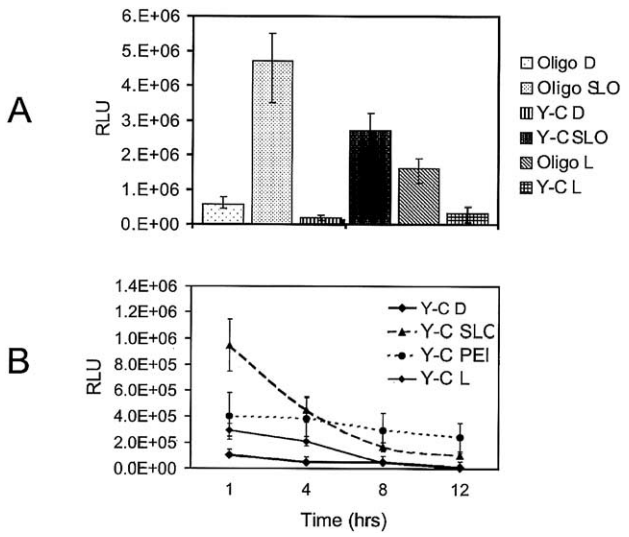

FIG. 4. Cytoplasmic and mitochondrial uptake of free oligonucleotides or PPO-complexes. A: Cytoplasmic uptake of 1 μM free FAM-labeled oligonucleotide (Oligo) or the oligonucleotide hybridized to the Y-conjugate (Y-C) into myoblasts transformed by direct exposure (D), permeabilization with streptolysin-O (SL-O) or encapsulation in liposomes (L). Uptake was measured in relative light units (RLU) of cytoplasmic fluorescence 2 hrs after transformation. B: Mitochondrial uptake of PPO-complexes (20 nM) measured as fluorescence per mitochondrial unit over time. Myoblasts were transformed with Y-conjugate/PPO- complexes (Y-C) by direct exposure (D), Streptolysin-O permeabilization (SL-O), aggregation with PEI (PEI) or by liposome encapsulation (L).

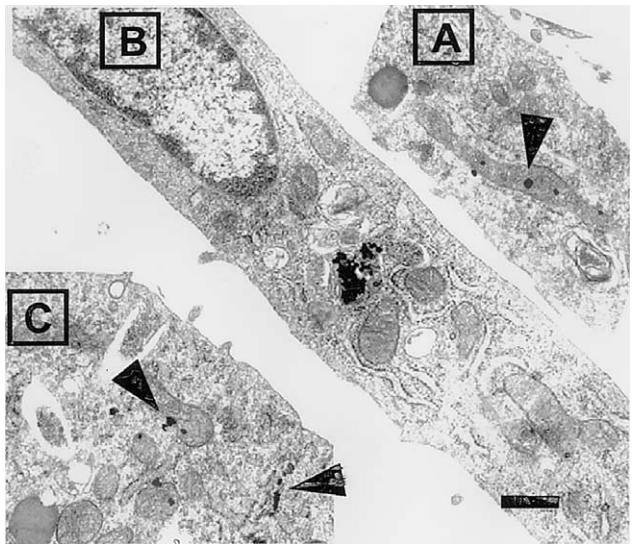

FIG. 5. Ultrastrucural localization of gold-labeled PPO-complexes in cultured cells. Myoblasts were transformed with PEI-PPO-aggregates containing the Y-conjugate hybridized to a gold-labeled oligonucleotide (A and C) or PEI-PPO-aggregates containing no targeting peptide (B). Electron micrographs were acquired from cross-sectioned myoblasts 4 hours after transformation. Arrowheads show silver-enhanced Undecagold™-particles. 14,000 × magnification. Bar length: 200 μm.

MATERIALS AND METHODS

PNA-peptide conjugates. The PNA-targeting peptide conjugates were synthesized by Research Genetics (Huntsville, Alabama), using PNA-monomers, activator, and resins from Perseptive Biosystems (Framingham, Maryland). PNAs were synthesized using solid phase chemistry (23), ending in two "Ado"-linker molecules (8-amino-3, 6-dioxa-octanoic acid). The mitochondrial targeting peptides were then extended from these spacers by solid-phase Fmoc protein chemistry (24). Conjugates (Table 1) were purified by RP-HPLC (25) and analyzed by MALDI-TOF MS (26).

M-conjugate. The "mouse," mitochondrial thiolase gene, 17 amino-acid pre-sequence (27) was conjugated to a 13 base PNA complementary to nucleotide pairs (nps) 15986–15998 of the *Mus musculus* mtDNA (28).

Y-conjugate. The "yeast" (*Saccharomyces cerevisae*), cytochrome-c oxidase subunit IV (COX IV) gene, 15 amino-acid pre-sequence (29) was coupled to a 13 base PNA molecule complementary to nps 3871–3883 of the plasmid PCR 2.1 (Stratagene; La Jolla, California).

SCR-conjugate. A "scrambled" peptide sequence of the same length as the M-chimera peptide was coupled to a PNA complementary to the mouse mtDNA nps 15986–15998.

W/o-conjugate. A PNA molecule "without" pre-peptide was synthesized with 13 bases PNA complementary to nps 3871–3883 of pPCR 2.1.

To identify the conjugates in gel systems, the peptide part was labeled with the fluorescent probe FQ (3-(2-furoyl) quinoline-2-carboxaldehyde) (Atto-Tag™, Molecular Probes; Eugene, Oregon). Reaction products were purified by HPLC (see *"Synthesis and Purification of Constructs"*).

Oligonucleotides and constructs. Oligonucleotides (IDT; Coraville, Idaho) were synthesized complementary to the PNA and extended for 3 to 5

doi:10.1016/S1525-0016(03)00037-6

nucleotides beyond the PNA sequence at the 5′ end (Table 1). 5′ ends of oligonucleotides were modified by C6 S-S phosphoramidite coupled to either FAM (5-carboxyfluorescein), Digoxigenin (DIG) (Roche Molecular Biochemicals; Indianapolis, Indiana) or Monomaleimido-Undecagold® (Nanoprobes™; Yaphank, New York). 5′ end thiolated oligonucleotides labeled with Undecagold® (30) were purified by DEAE Ion exchange chromatography (Amersham Pharmacia Biotech; Piscataway, New Jersey) and analyzed by denaturing TBE-Urea gel electrophoresis (31).

Synthesis and purification of PNA-peptide/oligonucleotide (PPO) complexes. All chemicals were obtained from Aldrich/Sigma (St. Louis, Missouri) unless stated otherwise. The PNA-peptide conjugates (20 nM) suspended in 0.05% Tween 20, 10 mM Tris-Cl and 10 mM KCl, pH 7.4 were heated to 75°C and then added to labeled oligonucleotides (2 mM). After incubation at 75°C for 5 min the reaction was cooled to RT at 1.5°C/min.

Reaction products were purified by RP-HPLC ("System Gold Nouveau" Beckman; Fullerton, California) using a Octadecyl-4PW C18 RFLP column (Rohmhaas/Tosohaas; Montgomeryville, Pennsylvania). Separations were performed in medium A {50 mM TEAA/H_2O pH 5.3 (Pierce; Rockford, Illinois)}, with a gradient of 5%–100% medium B {50 mM TEAA/Acetonitrile (Burdick&Jackson; VWR; Atlanta, Georgia)}. Fluorescent-labeled reaction products were separated by 15% TBE-Urea gel electrophoresis with a MultiMark™ standard (Invitrogen; Carlsbad, California), and analyzed by scanning fluorescence spectrophotometry (FluoroImager 595, Molecular Dynamics; Sunnyvale, California). Purity of DIG-labeled reaction products separated as above and transferred onto PVDF-Membranes was confirmed by western blot (Western Breeze™; Invitrogen), using an anti-DIG antibody (Roche).

Gold-conjugated complexes, containing gold-labeled oligonucleotides were separated in 15% TB-EDTA gel systems and detected by silver staining (Silver Stain Plus™, Biorad; Hercules, California).

Cell free import-assays. Mitochondria from liver of SV129 mice were prepared by differential centrifugation followed by Percoll® gradient purification (32). Respiration-competent mitochondria (200 μg) were incubated with 50 nM DIG-labeled PPO-complex in the presence of a standard mitochondrial import reaction mixture (33) or with reaction mixtures with modified mitochondrial energetic capacities (34). After incubation, unincorporated PPO-complexes were removed and mitochondria were repurified by Percoll® gradient centrifugation and subfractionated into outer membrane, inner membrane and matrix using digitonin (Roche) and differential centrifugation (35,36). Fractions were routinely identified by the appropriate marker enzymes and then analyzed on a 4–20% Tris-Glycine-SDS polyacrylamide gel system (Invitrogen). DIG-labeled oligonucleotides were detected using anti-DIG antibodies and Western blots.

Cell lines, in vitro transformation. The mouse muscle myoblastoid cell line C2C12 (ATTC®; Rockville, Maryland/No.: CRL-1772) was expanded (37) and 4×10^4 cells were seeded into 8-cell chamber slides™ (Nalgene Nunc, Fisher; Pittsburgh, Pennsylvania) 24 h before the experiment. Prior to transformation, the cells were washed 3 times in PBS. Then 50 μl of the transformation medium was added. For transformations without cytosolic up-take agents, 1 nM-1 μM of the FAM-labeled Y-construct was used. For transformations with agents to improve cytosolic uptake, 20 nM of fluorochrome-labeled and 250 pM gold-labeled PPO-complexes were used.

Cationic liposomes. Liposomes were prepared using DOTAP/DOPE formulations, Fugene™ 6 (Roche) and Escort™ (Sigma/Aldrich). Molecular ratios of the cationic lipids were adjusted to match the cell-type and the size of the nucleic acid component of the PPO-complexes. Cells were transformed using liposomes in Opti-Mem™ serum free medium (Gibco.Brl; Grand Island, New York) for 1 h. Following transformation, the cells were washed 3 times in PBS and incubated in standard growth medium.

Polyethylenimine (PEI). Aggregates were formed between the PPO-complexes and PEI (Sigma/Aldrich) using branched PEI with molecular weights of 750 kDa, 25 kDa and 700 Da to assess cytotoxicity and transformation efficacy. Optimal conditions employed 25 kDa PEI in 20 mM HEPES buffered saline (HBS) with nitrate (PEI) to phosphate (DNA) ratios (38) of 10. Complexes were prepared fresh for each experiment, and incubated with the cells in standard growth medium.

Streptolysin-O (SL-O). The optimal concentration of activated SL-O (Sigma/Aldrich) for permeabilization of the cells was established prior to each experiment (39). Activated SL-O (200–350 U/ml) and 10 nM of the PPO-complex were incubated with PBS-washed cells in Opti-Mem™ serum free medium at 37°C for 10 min. The permeabilized cells were resealed by adding 10 Vol. of pre-warmed growth medium.

Undecagold™. Adherent mouse C2C12 cells were transformed with Undecagold™-labeled PPO-complexes for 4 hours in the presence of SL-O or PEI. Cells were then removed from their substrate, washed and prepared for transmission electron microscopy (40,41) (EM Facility, Dept. of Biochemistry/Emory University).

Data acquisition. Following transformation, cells were incubated for 1–12 h in standard growth medium. The intracellular location of the fluorescent-labeled PPO-complexes was determined by counterstaining the transformed cells with organelle-specific dyes: 200 nM Mitotracker® CMX-Ros and 100 nM Lysotracker™ Red DND-99 (Molecular Probes) for 30 min. Cells were then washed, fixed in 3.5% paraformaldehyde/1.5% glutaraldehyde (Sigma) and mounted for fluorescence microscopy (AntiFade™, Molecular Probes).

Samples were analyzed by fluorescence microscopy (Axiovert™, Zeiss, St Louis, Missouri) using 40x and 100x objectives and two separate dye specific filter sets (FITC Filter set 17, Zeiss/HQ TRITC Filter set, Chroma Tech.; Brattleboro, Vermont). After controlling for light microscope focus, the images for the two fluorophores were collected sequentially with an Optronics™ (Goleta, California) DEI-470 CCD video camera system at 1240×1024 pixels. Digitized images were processed using *Mediagrabber*™ image processing software (Raster Ops; Indianapolis, Indiana) and superimposed using Adobe Systems Inc. software.

Statistical analysis. Semi-quantitative evaluation of the amount of fluorescent probe associated with the mitochondria was performed by digital image analysis (Image J; http://rsb.info.nih.gov/ij/docs). The ratio of mitochondrial green fluorescence of the labeled PPO-complex versus red fluorescence of Mitotracker® was calculated and the results of twenty cells were averaged for each experiment.

ACKNOWLEDGMENTS

This work was supported by NIH grants NS21328, NS41850, AG13154, HL64017 and an Ellison Foundation Senior Investigator Grant awarded to D.C.W.

RECEIVED FOR PUBLICATION SEPTEMBER 18, 2002; ACCEPTED JANUARY 27, 2003.

REFERENCES

1. Butow, R. A., Henke, R. M., Moran, J. V., Belcher, S. M., and Perlman, P. S. (1996). *Meth. Enzymol.* **264:** 265–78.
2. Collombet, J. M., Wheeler, V. C., Vogel, F., and Coutelle, C. (1997). *J. Biol. Chem.* **272:** 5342–7.
3. Irwin, M. H., Johnson, L. W., and Pinkert, C. A. (1999). *Trans. Res.* **8:** 119–23.
4. Vestweber, D., and Schatz, G. (1989). *Nature* **338:** 170–2.
5. Seibel, P., *et al.* (1995). *Nucl. Acids Res.* **23:** 10–7.
6. Schatz, G. (1996). *J. Biol. Chem.* **271:** 31763–6.
7. Geromel, V., *et al.* (2001). *Antisense & Nucleic Acid Drug Development* **11:** 175–80.
8. Nielsen, P. E., Egholm, M., Berg, R. H., and Buchardt, O. (1991). *Science* **254:** 1497–500.
9. Chinnery, P. F., *et al.* (1999). *Gene Ther.* **6:** 1919–28.
10. Jensen, K. K., Orum, H., Nielsen, P. E., and Norden, B. (1997). *Biochemistry* **36:** 5072–7.
11. Demidov, V. V., *et al.* (1994). *Biochem. Pharmacol.* **48:** 1310–3.
12. Tyler, B. M., *et al.* (1999). *Proc. Natl. Acad. Sci. USA* **96:** 7053–7058.
13. Beltinger, C., *et al.* (1995). *J. Clin. Invest.* **95:** 1814–23.
14. Felgner, P. L., *et al.* (1987). *Proc. Natl. Acad. Sci. USA* **84:** 7413–7.
15. Godbey, W. T., Wu, K. K., and Mikos, A. G. (1999). *J. Control Release* **60:** 149–60.
16. Dunlap, D. D., Maggi, A., Soria, M. R., and Monaco, L. (1997). *Nucl. Acids Res.* **25:** 3095–101.

17. Walev, I., Palmer, M., Valeva, A., Weller, U., and Bhakdi, S. (1995). *Infect. Immun.* **63:** 1188–94.
18. Bhakdi, S., *et al.* (1993). *Med. Microbiol. Immunol. (Berl)* **182:** 167–75.
19. Schwartz, M. P., and Matouschek, A. (1999). *Proc. Natl. Acad. Sci. USA* **96:** 13086–90.
20. Waltner, M., Hammen, P. K., and Weiner, H. (1996). *J. Biol. Chem.* **271:** 21226–30.
21. Blanc, H., Adams, C. W., and Wallace, D. C. (1981). *Nucl. Acids Res.* **9:** 5785–95.
22. Wallace, D. C. (1986). *Somatic Cell & Molecular Genetics* **12:** 41–9.
23. Christensen, L., *et al.* (1995). *J. Pept. Sci.* **1:** 175–83.
24. Aldrian-Herrada, G., *et al.* (1998). *Nucl. Acids Res.* **26:** 4910–6.
25. Mayfield, L. D., and Corey, D. R. (1999). *Anal. Biochem.* **268:** 401–4.
26. Butler, J. M., Jiang-Baucom, P., Huang, M., Belgrader, P., and Girard, J. (1996). *Anal. Chem.* **68:** 3283–7.
27. Murakami, K., Tanase, S., Morino, Y., and Mori, M. (1992). *J. Biol. Chem.* **267:** 13119–22.
28. Bibb, M. J., Van Etten, R. A., Wright, C. T., Walberg, M. W., and Clayton, D. A. (1981). *Cell* **26:** 167–80.
29. Maarse, A. C., *et al.* (1984). *EMBO J.* **3:** 2831–7.
30. Alivisatos, A. P., *et al.* (1996). *Nature* **382:** 609–11.
31. Skripkin, E., *et al.* (1993). *Bioconjugate Chemistry* **4:** 549–53.
32. Gasnier, F., *et al.* (1993). *Anal. Biochem.* **212:** 173–8.
33. Gasser, S. M., Daum, G., and Schatz, G. (1982). *J. Biol. Chem.* **257:** 13034–41.
34. Wachter, C., Schatz, G., and Glick, B. S. (1994). *Molecular Biology of the Cell* **5:** 465–74.
35. Schnaitman, C., and Greenawalt, J. W. (1968). *J. Cell. Biol.* **38:** 158–75.
36. Pedersen, P. L., *et al.* (1978). *Methods Cell. Biol.* **20:** 411–81.
37. Yaffe, D., and Saxel, O. (1977). *Nature* **270:** 725–7.
38. Ogris, M., *et al.* (1998). *Gene Ther.* **5:** 1425–33.
39. Barry, E. L., Gesek, F. A., and Friedman, P. A. (1993). *Biotechniques* **15:** 1016–1018 1020.
40. Humbel, B. M., Sibon, O. C., Stierhof, Y. D., and Schwarz, H. (1995). *J. Histochem. Cytochem.* **43:** 735–7.
41. Moses, R. L., and Claycomb, W. C. (1982). *Am. J. Anat.* **164:** 113–31.